Talanta 125 (2014) 301–305

Contents lists available at ScienceDirect

Talanta

journal homepage: www.elsevier.com/locate/talanta

A symmetric pseudo salen based turn-on fluorescent probe for sensitive detection and visual analysis of zinc ion

Huan Yu [a,1], Tao Yu [b,1], Mingtai Sun [a], Jian Sun [a,c], Shan Zhang [a,c], Suhua Wang [a,c,*], Hui Jiang [b,**]

[a] Institute of Intelligent Machines, Chinese Academy of Sciences, Hefei 230031, PR China
[b] Beijing Institute of Pharmaceutical Chemistry, State Key Laboratory of NBC Protection for Civilian, Beijing 102205, PR China
[c] Department of Chemistry, University of Science & Technology of China, Hefei 230026, PR China

ARTICLE INFO

Article history:
Received 24 December 2013
Received in revised form
1 March 2014
Accepted 10 March 2014
Available online 17 March 2014

Keywords:
Pseudo salen moiety
Zinc ion
Fluorescent probes
Coordination modes
Visual detection

ABSTRACT

A turn-on fluorescence probe for zinc ion has been synthesized, which contains a symmetric pseudo salen moiety as zinc recognition site. The multidentate salen ligand chelates with zinc ions, and generates the rigidity of the zinc complex, which subsequently results in a dramatic fluorescence enhancement of the probe. Mass spectral and spectroscopic results reveal that the reaction proceeds rapidly in a 1 to 1 stoichiometric manner to form a clean zinc complex. We have demonstrated that the fluorescence probe not only has high selectivity for zinc ion over other biological relevant ions but also shows high sensitivity for zinc ion with a detection limit of 83 nM. A fluorescence test paper has been developed by incorporating the probe on a polyamide fiber paper. The fluorescence color of the test paper became bright green–yellow under UV lamp when water sample containing zinc ions was dropped on it, suggesting its potential application in the measurement of zinc ions.

1. Introduction

As an essential trace element in biological systems, zinc ion (Zn^{2+}) plays an important role in physiological processes, for example, it is a structural or catalytic cofactor for some enzyme and receptor regulation function [1,2]. It is also closely associated with biosynthesis of DNA, RNA and common proteins. Failure of maintain zinc ions homeostasis in body can cause several neurological diseases such as Alzheimer's disease, Parkinson's disease, diabetes, depression and dysplasia [3–5]. Real-time monitoring the uptake, accumulation, trafficking and efflux of zinc ions is of great importance for diagnosis and prophylaxis of such diseases. Therefore, the development of new molecular probes for sensitive and selective detection of zinc ion has been a concern of chemists.

The current methods for zinc ion detection include surface enhanced raman scattering (SERS) [6], electrochemistry [7,8], absorption and fluorescence spectrometry [9]. The method based on SERS uses dithiocarbamate as a substrate and supports the detection of zinc ions at trace level [10]. In recent years, some zinc fluorescent probes have been reported for the detection of zinc ions. These probes generally comprise a chelating moiety and a fluorophore group, which are responsible for the recognition of zinc ions and the generation of fluorescence signal variation, respectively [11–15]. The optical properties of these organic probes are dependent on the substituted groups surrounding the fluorophore moiety. In these probes, the pyrazoline, 2,2′-dipicolylamine (DPA) [16–17], porphyrin [18], bipyridine, quinoline [19–22] and pyridine groups are often used as zinc ion chelators. Some of these probes show cross sensitivity toward other heavy metal ions such as Hg^{2+} and Cd^{2+}, which degrades the selectivity. So, it remains a challenge to develop sensitive and selective fluorescent probes for Zn^{2+}, which has a specific zinc ion chelating ability. Herein, we report a new sensitive and selective fluorescent probe for Zn^{2+} detection, which was synthesized by reacting dansyl chloride with a pseudo salen moiety containing amino groups. Dansyl chloride [23–25] is often used as a derivatizing agent and is intrinsically weakly fluorescent. Upon rapid reaction with the amino groups, a sulfamide derivative formed and its fluorescence property is dependent on the molecular structure. The salicylaldehyde-derived pseudo salen receptor can efficiently bond with zinc ions

* Corresponding author at: Institute of Intelligent Machines, Chinese Academy of Sciences, Hefei 230031, PR China. Tel.: +86 551 6559 1812; fax: 86 551 6559 1156.
** Corresponding author at: Beijing Institute of Pharmaceutical Chemistry, State Key Laboratory of NBC Protection for Civilian, Beijing 102205, PR. China.
E-mail addresses: shwang@iim.ac.cn (S. Wang), jiangtide@sina.cn (H. Jiang).
[1] These two authors contributed equally to this work.

http://dx.doi.org/10.1016/j.talanta.2014.03.011
0039-9140/

and the dansyl fluorophore provides fluorescence signal. The probe has been demonstrated to selectively and sensitively respond to Zn^{2+} in a wide concentration range.

2. Experimental

2.1. Materials and chemicals

All reagents were purchased from commercial suppliers and used without further purification. Solvents were purified by standard methods prior to use. All the solutions were prepared with water purified by a Millipore water purification system (18.2 MΩ cm). $CaCl_2$, $CuCl_2 \cdot 2H_2O$, $BaCl_2$, $FeCl_3 \cdot 6H_2O$, $MgCl_2 \cdot 6H_2O$, $NiCl_2 \cdot 6H_2O$, $MnSO_4 \cdot 1H_2O$, $CdCl_2 \cdot 2.5H_2O$, $CoCl_2 \cdot 6H_2O$, $ZnCl_2$, $Pb(NO_3)_2$ and$Hg(NO_3)_2$ were used to prepare metal ion stock solutions. $CDCl_3$ were used to record ^1H NMR spectra.

2.2. Apparatus

The UV–vis absorption spectra were recorded with a Shimadzu UV-2550 spectrometer at room temperature. Fluorescence measurements were performed on a Perkin-Elmer LS-55 luminescence spectrometer (Llantrisant, UK) equipped with a quartz cell (1 cm × 1 cm). The slit widths for excitation and emission were both 10 nm. ^1H NMR spectra were recorded on a Brucker Advance 400 NMR spectrometer. Mass spectra were obtained on a Thermo Prpteome X-LTQ MS mass spectrometer in ES positive and negative mode. Photographs were taken by a Canon 350D digital camera. Thin layer chromatography analysis was performed on silica gel plates and column chromatography was conducted over silica gel (mesh 200–300).

2.3. Synthesis of compounds 2,2′-(1E,1′E)-(2,2-azanediylbis(ethane-2,1-diyl)bis(azan -1-yl-1-ylidene))bis(methan-1-yl-1-ylidene) dipnenol, TAS

Diethylenetriamine (2 mmol, 200 mg) was dissolved in CH_3OH (6 ml) at room temperature, salicylaldehyde (2.5 mmol, 310 mg) was then added to form a clear solution. The solution was further stirred for 2 h at room temperature. The solvent was then removed under reduced pressure to obtain the crude product, which was further purified by column chromatography on silica (CH_2Cl_2: CH_3OH=9:1) to yield pure yellow oil product TAS (430 mg, 70.5% yield).

2.4. Synthesis of compounds [5-(dimethylamino)-N,N-bis(2-((E)-2-hydroxybenzy lideneamino)ethyl)naphthalene-1-sulfonamide], DS-TAS

A portion (200 mg, 0.6 mmol) of compound TAS was mixed with dansyl chloride (205 mg, 0.7 mmol) in 6 mL of CH_2Cl_2 and several drops of pyridine were added, followed by stirring for 2 h at room temperature. The reaction mixture was then filtered and the filtrate was dried by rotary evaporator under reduced pressure. The resulting residue was subjected to column chromatography on silica (CH_2Cl_2:CH_3OH=30:1) and finally a yellow–green solid, DS-TAS (261.1 mg, 80.2% yield). ESI-MS: 543.14 (M^-). ^1H NMR (400 MHz, $CDCl_3$) δ 12.82 (s, 2H), 8.47 (d, J=8.5 Hz, 1H), 8.2–8.12 (m, 2H), 7.96 (s, 2H), 7.47–7.42 (m, 1H), 7.37 (ddd, J=7.8, 6.8, 3.8 Hz, 1H), 7.22 (ddd, J=8.4, 7.3, 1.7 Hz, 2H), 7.05 (d, J=7.1 Hz, 1H), 7.01 (dd, J=7.6, 1.6 Hz, 2H), 6.84 (d, J=8.3 Hz, 2H), 6.77 (td, J=7.5, 1.1 Hz, 2H), 3.64–3.54 (m, 7H), 2.80 (d, J=4.8 Hz, 5H).

2.5. Fluorescence experiments

A stock solution of DS-TAS (1 mM) in ethanol was prepared. The working solution of DS-TAS (500 nM) was prepared by diluting 1 μL of the DS-TAS stock solution in 2 mL ethanol. The metal ion solutions were added into the mixture followed by recording the fluorescence spectra. Equimolar solutions of DS-TAS and Zn^{2+} were prepared first for the Job's plot experiment. The two solutions were then mixed in standard volume and proportion in order to keep the total concentration of probe and Zn^{2+} constant of 500 nM. All fluorescence spectra were recorded in the range from 420 nm to 750 nm using a 360 nm excitation wavelength and a 500 nm/min scan rate.

2.6. Preparation of fluorescence test paper

2 μL of DS-TAS (5 μM) was dripped on a piece of polyamide fiber paper to form a spot about 5 mm in diameter, followed by drying under air. The spot was nearly colorless under a 365 nm UV lamp. In order to detect Zn^{2+}, 2 μL of Zn^{2+} with different concentrations from 0.5 μM to 5 μM was dropped on the center of the spot. Then after the spot was air-dried under room temperature, the indicating paper was put under a UV lamp with excitation wavelength of 365 nm to observe the change of fluorescence color.

3. Results and discussion

3.1. Characterization of DS-TAS

The fluorescence probe, DS-TAS, was obtained in high yield through a simple two-step reaction modified from a literature [26], as shown in Scheme S1. The probe contains two functional segments, the pseudo salen moiety as the analyte-sensitive receptor and dansyl moiety as fluorophore reporter, whose fluorescence quantum yield is dependent on the conformation of salen moiety. The chemical structure is confirmed by ESI-MS (Fig. S1) and ^1H NMR (Fig. S2). The ESI-MS spectrum shows a peak at m/z 543.14 in negative mode which matches perfectly with the calculated molecular weight of [DS-TAS].

3.2. Spectroscopic properties of DS-TAS

The UV–vis spectrum of the probe in ethanol shows two absorption bands at 254 and 320 nm. The spectrum changes gradually upon the addition of zinc ion as shown in Fig. 1. The two absorption bands decrease and finally disappear as the amount of Zn^{2+} added increases, accompanied by the appearance of three new absorption peaks at 225, 270 and 360 nm. The new absorption peaks gradually increase and finally reach their plateaus when one molar equivalent of Zn^{2+} was added. The red shift of the absorption bands can be attributed to the zinc coordination and the formation of a planar complex. It can be seen that four isosbestic points at 250, 262, 291 and 335 nm produced, which correspond to the clear formation of zinc complex. The well-defined isosbestic points clearly indicate the formation of a new complex in equilibrium with the free DS-TAS ligand. The appearance of the absorption band at 360 nm indicates the formation of DS-TAS–Zn complex and isomerisation of the C=N bond. DS-TAS contains both hydroxyl and C=N groups that are well-known to be involved in metal ions coordination. Upon addition of Zn^{2+}, the acidities of phenolic hydroxyl is enhanced and therefore an excited-state intra/inter molecular proton transfer (ESPT) channel might be opened. A new absorption band at 360 nm arising from

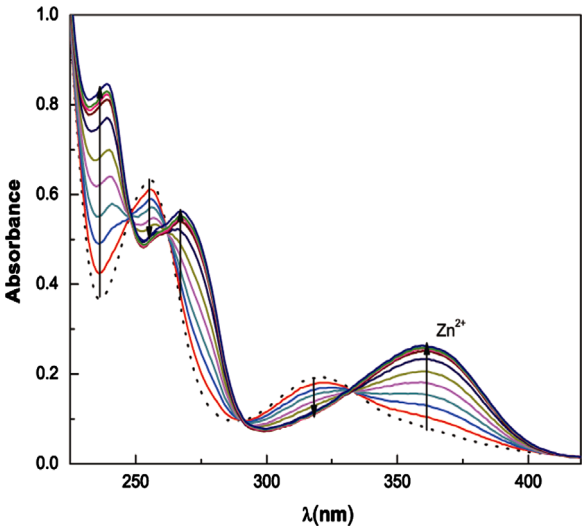

Fig. 1. UV–vis absorption spectra responses of a 20 μM solution of DS-TAS in ethanol upon addition of different amounts of Zn^{2+} (0–20 μM). The absorption band at 320 nm decreased gradually and a new absorption band appeared at 360 nm as the amount of Zn^{2+} increased. The arrows indicate the signal variation trends upon Zn^{2+} adding.

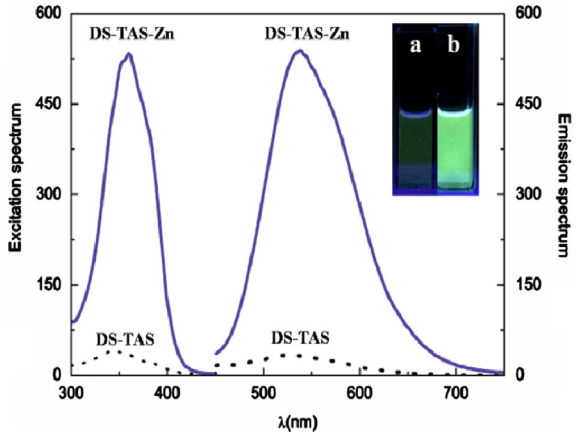

Fig. 2. Excitation spectra and emission spectra of DS-TAS (500 nM) in ethanol. The dot line and solid line are the excitation and emission spectra of DS-TAS and DS-TAS–Zn, respectively. The inset shows the fluorescence images of 500 nM DS-TAS (a) and DS-TAS-Zn (b) under a 365 nm UV lamp.

chelation with Zn^{2+} illustrates the formation of organic-metal complex.

The fluorescence responses of DS-TAS to zinc ions were also studied at concentrations much lower than that used in UV absorption study. Fig. 2 shows the excitation and emission spectra of DS-TAS in the absence and presence of zinc ions. Clearly, the fluorescence quantum yield of DS-TAS increases greatly upon the addition of zinc ion. The emission band of DS-TAS at 523 nm is initially very weak and increases more than 10 times after the addition of one molar equivalent zinc ion, which implies the formation of zinc complex, DS-TAS–Zn.

Clearly, chelation of zinc ion to the probe results in the enhancement of fluorescence quantum yield of the fluorophore. This property was thus utilized for visual detection of zinc ions, which was demonstrated in the Fig. 2 inset. The solution of DS-TAS probe initially exhibited weak fluorescence under a UV lamp. However, a bright yellowish green fluorescence was turned on by the addition of zinc ion. This clearly shows that the weakly fluorescent probe DS-TAS can be turned-on when exposed to zinc ion.

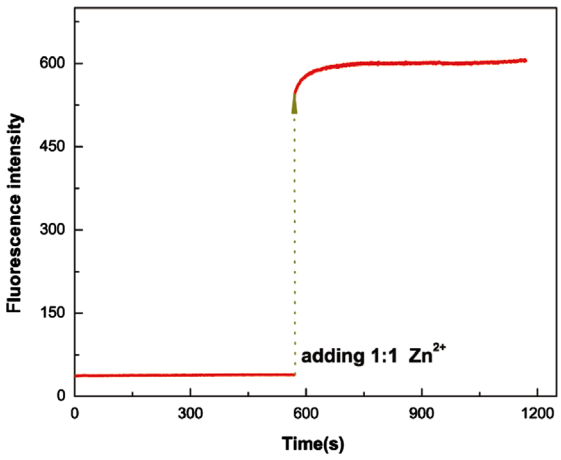

Fig. 3. Photostability of DS-TAS (500 nM) in the absence and in the presence of one equiv. of Zn^{2+}. Fluorescence intensity was recorded at 535 nm in ethanol with an excitation wavelength of 360 nm. (The photostability was investigated by irradiating its solution under a Xenon light source with a power of 20 kW).

Both the probe DS-TAS and its zinc complex exhibit good photostability, as illustrated in Fig. 3. It can be seen that the fluorescence intensity of the probe in the absence of zinc ion maintains constant under continuous irradiation at 360 nm for 10 min. When one molar equivalent zinc ion is added, the fluorecence intensity rapidly bursts and reaches a plateaue in seconds. Furthermore the fluorescence intensity keeps constant under illumination for ten more minutes. The results suggest the high photostability of the weakly fluorescent probe and the highly fluorescent complex of DS-TAS–Zn. The fluorescence enhancement of DS-TAS by zinc ion can be attributed to ESPT and chelation-enhanced fluorescence (CHEF) [27,28]. The symmetric pseudo salen moiety is often known as excellent multidentate ligand for transition metal ions. Chelating with zinc ion helps the skeleton of fluorophore to be rigid and induces the CHEF. As shown in Fig. S3, the presence of Cu^{2+}, Co^{2+} and Ni^{2+} induce little absorption variation but has no effect on fluorescence intensities.

3.3. Fluorescence titration and stoichiometric reaction

The dose-response of the fluorescence of the probe to Zn^{2+} (0 to 1 equiv.) was carefully examined, as shown in Fig. 4. A linear relationship was observed, which enables the quantitative determination of Zn^{2+}. The limit of detection (LOD) was found to be 83 nM based on the definition of three times deviation of blank signal by using the curve fitting of Fig. 4B. Continuous titration of Zn^{2+} with more than 1 equiv. leads to no further enhancement of the fluorescence intensity. In order to detect Zn^{2+} at higher concentrations, the performance of the probe at higher concentration was carefully studied (Fig. S4). The fluorescence intensity was also increased gradually and in proportional to the concentrations of Zn^{2+} in the range from 0.5 μM to 6 μM. A similar linear relationship ($R=0.9939$) can be obtained with a limit of detection of 0.64 μM (Fig. S4B). This detection limit obtained at higher probe concentration is higher than that at lower concentration. This is due to that higher probe concentration brings high fluorescence background.

The stoichiometric reaction of the probe DS-TAS with zinc ion was determined by the Job's plot and ESI-MS spectrum (Fig. 5 and Fig. S5). The Job's plot shows that the maximum fluorescence intensity reaches when the molar fraction of DS-TAS is around 0.5, which clearly suggests a 1 to1 stoichiometric ligand–metal binding (inset in Fig. 5). The ESI-MS spectrum of the complex displays a peak at m/z 607.13 as $[DS\text{-}TAS\text{–}Zn\text{–}H]^+$, in consistent with the

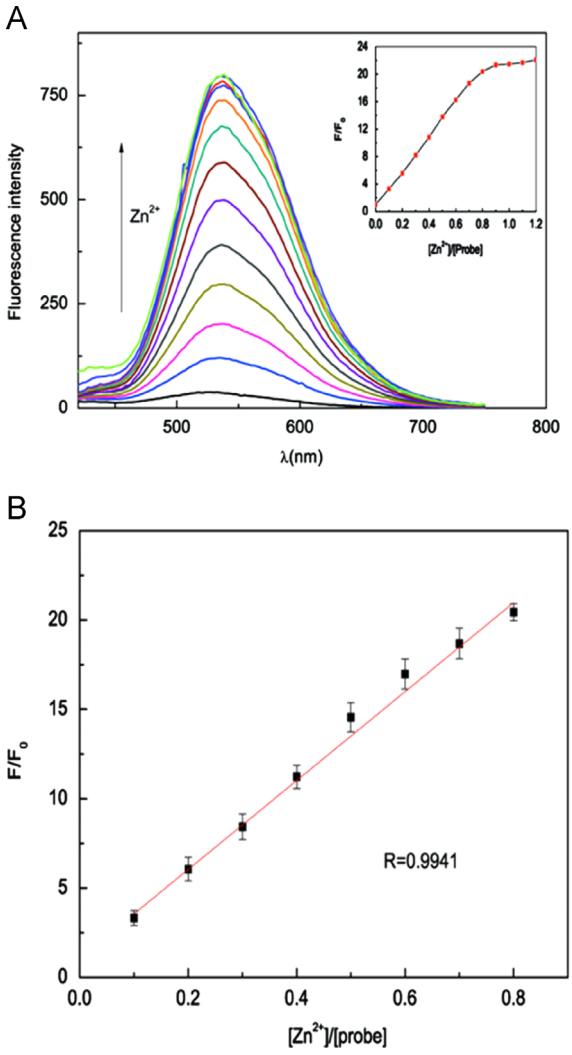

Fig. 4. (A) Fluorescence enhancement of probe DS-TAS upon the addition of Zn^{2+} (0–0.6 μM) in ethanol. Inset: changes of fluorescence intensity of DS-TAS with different amounts of Zn^{2+} at 535 nm. F_0 and F were the fluorescence intensity of DS-TAS (500 nM) in the absence and in the presence of Zn^{2+}, respectively. (B) Plot of fluorescence enhancement efficiency of the DS-TAS solution as a function of the Zn^{2+} concentration. The fluorescence spectra were recorded with excitation at 360 nm.

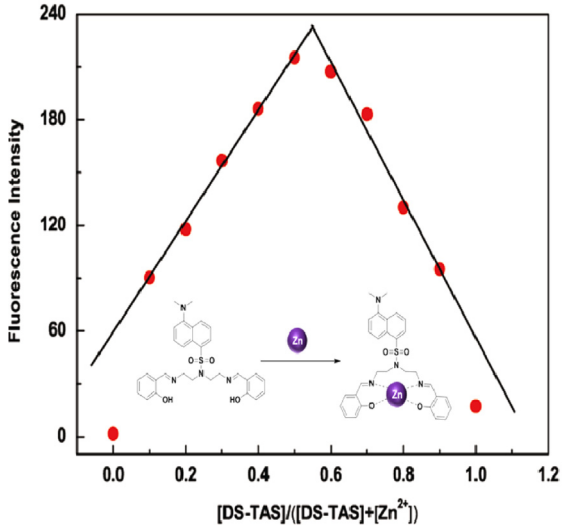

Fig. 5. Job's plot for the binding of DS-TAS with Zn^{2+} in ethanol as a function of the molar ratio as [DS-TAS]/([DS-TAS]+[Zn^{2+}]). The total constant concentration for DS-TAS and Zn^{2+} is 500 nM. Inset: the proposed binding mode of DS-TAS-Zn.

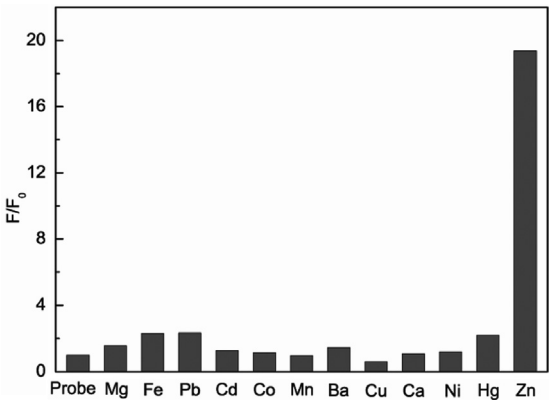

Fig. 6. Selectivity of the DS-TAS probe over other metal ions with the concentration of 500 nM. F_0 and F were the fluorescence intensity of DS-TAS (500 nM) in the absence and in the presence of each metal ions, respectively.

calculated value which further verifies the 1:1 stoichiometric binding between the ligand and zinc ion. These results confirm the chelation mode and the 1 to 1 stoichiometric reaction between the probe and zinc ion.

3.4. Metal ions selectivity and interference studies

The selectivity of the fluorescence probe among biological relevant metal ions was investigated by monitoring the fluorescence responses to the addition of various cations. Fig. 6 shows the enhancement of fluorescence intensity of the probe after addition of various metal ions. The results clearly show that these cations including Co^{2+}, Cu^{2+}, Ni^{2+}, Mn^{2+}, Ba^{2+}, Ca^{2+}, Mg^{2+} and Cd^{2+} have no enhancement effect on the fluorescence of the probe. While Hg^{2+}, Pb^{2+} and Fe^{3+} exhibit slight enhancement, it is still negligible when compared with Zn^{2+}. The results indicate the good selectivity for zinc ions over other cations.

The interference study was carried out in the presence of other cations with higher concentrations (Fig. S6). The results show that the presence of other cations does not interfere the fluorescence enhancement by Zn^{2+}. However Cu^{2+} shows quenching effect on the fluorescence turned-on by zinc ion, which could be due to the competition binding with the salen moiety. We further examined the interaction between Cu^{2+} and the probe before and after adding Zn^{2+} (Fig. S7). Experimental data show that Cu^{2+} has strong coordination ability and quenching properties, which induces fluorescence decrease before and after adding Zn^{2+}. The interference of Cu^{2+} can be avoided by a simple pretreatment using $Na_2S_2O_3$ to mask Cu^{2+} [29] (Fig. S8). These results manifest that DS-TAS exhibits good selectivity toward Zn^{2+} over most competing metal ions.

3.5. Fluorescence test paper for zinc ion detection

On-site visual determination of zinc ions is very useful for clinic diagnosis of zinc metabolism disorder related diseases. For this purpose, we immobilized the fluorescent probe on polyamide fiber paper to make zinc ion-indicating papers. The probe solution was evenly casted onto the paper, followed by air drying in dark at room temperature. The as-prepared indicating paper displays very weak green fluorescence background under a 365 nm UV lamp. For demonstration, 2 μL of zinc aqueous solution with different concentrations was carefully dropped on the indicating paper to form a series of stained spots. Clearly, bright green fluorescence spots on the test paper were observed under the illumination of

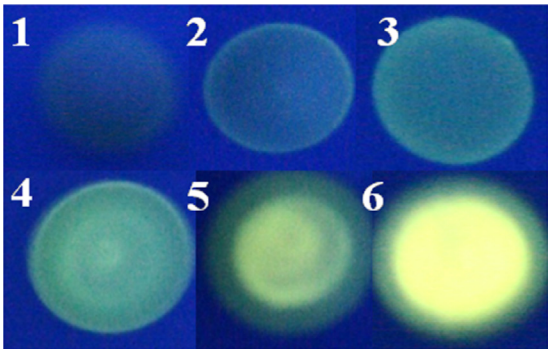

Fig. 7. Fluorescence images of DS-TAS spot on polyamide fiber paper after the addition of 2 μL of different concentrations of (from 1 to 6) 0 μM, 0.5 μM, 1 μM, 2 μM, 3 μM and 5 μM Zn^{2+}. All the images were taken under the illumination of a 365 nm UV lamp.

the UV lamp (Fig. 7). The brightness of the spots gradually increased as the amount of zinc ion applied was increased. The detection limit is defined as the least amount of Zn^{2+} used to turn on the fluorescence that can be observed independently by naked eye. The visual detection limit was thus estimated to be 500 nM.

4. Conclusion

A novel turn-on fluorescent probe for zinc ion detection has been synthesized. We have demonstrated that the fluorescent probe shows high sensitivity and selectivity for the detection of zinc ion, and the limit of detection is estimated to be 83 nM. The fluorescence turn-on mechanism of the weakly fluorescent DS-TAS involves a 1 to 1 stoichiometric reaction between the probe and zinc ion. A practical fluorescence test paper has been developed for the visual detection of zinc ion in aqueous samples and could be useful in clinical diagnosis.

Acknowledgments

This work was supported by the National Basic Research Program of China (2011CB933700), the Natural Science Foundation of China (Nos. 21173229, 21205120 and 21302187) and the Innovation Project of Chinese Academy of Sciences (KJCX2-YW-H29).

Appendix A. Supporting information

Supplementary data associated with this article can be found in the online version at http://dx.doi.org/10.1016/j.talanta.2014.03.011.

References

[1] P.D. Zalewski, I.J. Forbes, W.H. Betts, Biochem. J. 296 (1993) 403–408.
[2] X. Xie, T.G. Smart, Nature 349 (1991) 521.
[3] C.E. Outten, T.V. O'Halloran, Science 292 (2001) 2488.
[4] C.J. Frederickson, M.D. Hernandez, J.F. McGinty, Brain Res. 480 (1989) 317.
[5] A.I. Bush, W.H. Pettingell, G. Multhaup, M. Paradis, J.P. Vonsattel, J.F. Gusella, K. Beyreuther, C.L. Masters, R.E. Tanzi, Science 265 (1994) 1464.
[6] Y. Zhao, J.N. Newton, J. Liu, A. Wei, Langmuir 25 (2009) 13833–13839.
[7] K. Sołtyk, A. Łozak, M. Warowan-Grześkiewicz, Z. Fijałek, Acta. Pol. Pharm. 57 (2000) 261–266.
[8] K.P. Gong, M.N. Zhang, Y.M. Yan, L. Su, L.Q. Mao, S.X. Xiong, Y. Chen, Anal. Chem. 76 (2004) 6500–6505.
[9] M.L. Chen, J.W. Liu, B. Hu, M.L. Chen, J.H. Wang, Analyst 136 (2011) 4277–4283.
[10] H. Ko, S. Srikanth, V.V. Tsukruk, Small 4 (2008) 1576–1599.
[11] K.M. Hendrickson, J.P. Geue, O. Wyness, S.F. Lincoln, A.D. Ward, J. Am. Chem. Soc. 125 (2003) 3889–3895.
[12] A. Ajayaghosh, P. Carol, S. Sreejith, J. Am. Chem. Soc. 127 (2005) 14962–14963.
[13] K. Kiyose, H. Kojima, Y. Urano, T. Nagano, J. Am. Chem. Soc. 128 (2006) 6548–6549.
[14] B. Zhang, K.S. Cao, Z.A. Xu, Z.Q. Yang, H.W. Chen, W. Huang, G. Yin, X.Z. You, Eur. J. Inorg. Chem. 24 (2012) 3844–3851.
[15] P.W. Du, S.J. Lippard, Inorg. Chem. 49 (2010) 10753–10755.
[16] T. Hirano, K. Kikuchi, Y. Urano, T. Nagano, J. Am. Chem. Soc. 124 (2002) 6555–6562.
[17] C.C. Zhao, Y.L. Zhang, P. Feng, J. Chao, Dalton Trans. 41 (2012) 831–838.
[18] R.H. Yang, K.A. Li, K.M. Wang, F.L. Zhao, N. Li, F. Liu, Anal. Chem. 75 (2003) 612–621.
[19] D.A. Pearce, N. Jotterand, I.S. Carrico, B. Imperiali, J. Am. Chem. Soc. 123 (2001) 5160–5161.
[20] Y. Mikata, M. Wakamatsu, S. Yano, Dalton Trans. 3 (2005) 545–550.
[21] Y. Zhang, X.F. Guo, L.H. Jia, S.C. Xu, L.B. Zheng, X.H. Qian, Dalton Trans. 41 (2012) 11776–11782.
[22] J. Luo, W.S. Li, P. Xu, L.Y. Zhang, Z.N. Chen, Inorg. Chem. 51 (2012) 9508–9516.
[23] S.T. Ulu, Luminescence 27 (2012) 426–430.
[24] R.L. Soon, T. Velkov, F. Chiu, P.E. Thompson, R. Kancharla, K. Roberts, I. Larson, R.L. Nation, J. Li, Anal. Biochem. 409 (2011) 273–283.
[25] Z. Aydogmus, F. Sari, S.T. Ulu, J. Fluoresc. 22 (2012) 549–556.
[26] H.J. Gais, P.R. Bruns, G. Raabe, R. Hainz, M. Schleusner, J. Runsink, G.S. Babu, J. Am. Chem. Soc. 127 (2005) 6617–6631.
[27] X. Zhang, L. Guo, F.Y. Wu, Y.B. Jiang, Org. Lett. 5 (2003) 2667–2670.
[28] H. Lin, P.Y. Cheng, C.F. Wan, A.T. Wu, Analyst 137 (2012) 4415–4417.
[29] L. Wang, W.W. Qin, X.L. Tang, W. Dou, W.S. Liu, J. Phys. Chem. A. 115 (2011) 1609–1616.